Phase Transformation in the Ti-24%Al-12.5%Nb Alloy

Ass.Prof. S.L.DEMAKOV, Eng. L.S.STEPANOV, Prof. POPOV A.A.
Ural State Technical University, Russia , 620002 Ekaterinburg, Mira str., 19

ANNOTATION
The phase composition, structure, and properties of a high-temperature α_2 intermetallic-based superalloy and the crystallographic parameters of the phases contained in it were studied as a function of the quenching temperature and the time at quenching temperature. It was found that the O => $\alpha_2+\beta$ transformation is controlled by the redistribution of niobium between the phases and, therefore, the transformation rate is deter-mined by the thickness of initial O-phase plates. The deviations from Vegard's law for Ti-Al were found to be the same in hexagonal and cubic lattices.

INTRODUCTION

The α_2 superalloys are new promising high-temperature titanium alloys based on intermetallic compounds. These alloys are as good as nickel-based alloys in their high-temperature strength and have substantially smaller specific weight. The alloy structure contains several ordered phases such as hard but very brittle α_2 phase and rather ductile β (B2) and O phases[1-3].

The aim of this work was to outline the effects of quenching temperature and time at quenching temperature on the phase composition, structure, and properties of the α_2 titanium intermetallic-based superalloy and the crystallographic parameters of the phases that form in it. We considered the relationship between the phase transformations and the redistribution of alloying elements. In addition, we attempted to simulate the mechanism of the O =>α_2 +β transformation.

1. MATERIALS AND METHODS OF RESEARCH

Specimens of the α_2 superalloy of composition Ti-23.8 Al-12.4 Nb-1.2 Zr-0.7.Mo (at.%) were cut from a hot-rolled sheet (1.5 mm thick). The alloy was deformed at 900°C and then cooled in air. The specimens were studied in the initial state and after water-quenching from 750-1150°C in steps of 50 K; the lengths of time at quenching temperatures were 5, 30, and 60 min.

The microstructure of the alloy was examined in a JSM-35c scanning electron microscope with an accelerating voltage of 15 kV, and a JEM-200 CX transmission electron microscope with an accelerating voltage of 160 kV. X-ray diffraction examination was performed on a DRON-3 diffractometer and a URVT-2000 high-temperature apparatus at a voltage of 30 kV and a current of 30 mA (using filtered copper radiation). X-ray diffraction patterns were taken from the sheet plane and from the cross-sectional plane of the sheet at 2θ angles ranging from 25° to 90°. The lattice parameters were calculated from the (400), (260), and (042) lines for the O phase; from the (200) and (220) lines for the β phase and from the (202) and (220) lines for the α_2 phase. Vickers hardness was measured at a load of 50 N.

2. RESULTS

The phase identification by X-ray diffraction showed that the initial material consists of the 0 phase and traces of the β and α_2 phases. As was shown by electron micrographs, the internal structure of the grains consists of coarse and fine needle-like precipitates (Fig. 1a).

After quenching from temperatures below 850°C. the alloy consists predominantly of the O phase, small amounts of the β (B2) phase, and traces of the α_2 phase (regardless the time at quenching temperature). As the quenching temperature increases, the time of the solidsolution treatment (5, 30, or 60 min) affects the form of the curves shown in Figs. 2b and 2c. At small times, the 0 => α_2 + β transformation is observed in a relatively narrow temperature range (jumpwise). With increasing solution-treatment time, the temperature range of the 0 => α_2 + β transformation increases, and the temperature corresponding to the formation of the maximum amount of the α_2 phase decreases. The upper temperature boundary at which the α_2 lines disappear in the X-ray diffraction patterns decreases from 1150°C for t = 5 min to 1100°C for t = 30 min.

In addition to the above distinctions, we observed the following general features. At 750-900°C, the O

phase partially transforms to the β phase. With increasing quenching temperature, the O phase lattice parameters approach those of the α_2 phase (Fig. 3a); the volume fraction of the β (B2) phase increases, and its lattice parameters decrease (Fig.3c).

The electron micrographs of the quenched samples are presented in Figs. 1b-1f. Quenching from 850-950°C does not cause substantial changes in the intragranular structure of the initial metal (Fig. 1a). We note only a decrease in the volume fraction of the O-phase precipitates at the expense of their dissolution in the β (B2) matrix. Fine needles dissolve at 850 and 900°C, whereas the dissolution of coarser needles is intensified at higher temperatures.

For quenching temperatures of 1000-1050°C, the orthorhombic O phase inside the needles transforms to the hexagonal (DO_{19}) α_2 phase without any noticeable changes in the precipitate morphology (Figs. 1b). With increasing temperature, the O phase lattice parameters a and c decrease, and the parameter b/ 3 increases (Fig. 3a). The O-phase parameters a and b/ 3 approach the α_2 phase parameter a, and the O phase parameter c approaches the α_2 phase parameter c (note that in this case, the parameter c of the O phase decreases and that of the α_2 phase increases).

The decrease in the volume fraction of the α_2 phase with increasing quenching temperature is accompanied by changes in the axial ratio c/a and a decrease in the unit-cell volume of this phase (at Tq = 1050°C, Vuc=0.157 nm^3 and at Tq = 1100°C, Vuc =0.1565 nm^3. This is likely to be due to decreasing niobium content. As the quenching temperature increases to 1100°C, the α_2 phase particles inside grains dissolve almost completely (and irreversibly), and the resulting alloy structure consists mainly of the β (B2) solid solution. Isolated α_2 phase precipitates are observed mainly near grain boundaries (Fig. 1c).

According to the data obtained on the high-temperature URVT-2000 setup, the phase compositions in the high-temperature and as-quenched states are not the same. For example, in the samples quenched from temperatures below 1000°C, the high-temperature phase composition is not fixed by quenching. For these samples, the curves describing the volume fraction of the β phase are identical, and the α_2 phase content increases with increasing temperature at the expense of decreasing O phase content. The upper boundary of the O phase existence is about 930°C.

The data on the effect of the quenching temperature and the time at quenching temperature on the hardness of the alloy are shown in Fig. 4. These data are in good agreement with the data on the phase composition of the alloy. The total decrease in hardness is caused by the increased volume fraction of the β phase. A temporary stabilization of hardness is observed in the temperature range of the existence of the α_2 phase as the main strengthening phase in the alloy. However, since this range is determined by the duration of the solution treatment, the stabilization limits gradually shift, as is seen from Fig. 4.

3. DISCUSSION

Let us consider the distribution of the main alloying elements in the phases present in the α_2 superalloy. The aluminum content should be about 25% both in the O phase and in the α_2 phase [4]. The alloy under study contains 24% Al; therefore, it is reasonable to assume that the Al content in the β phase (if the volume fraction of this phase is noticeable) is close to that in other phases. Therefore, we assume that the aluminum redistribution does not play an important role in the phase transformations occurring in the alloy. In our opinion, it is the niobium redistribution that is the most important factor in our case.

As the temperature decreases relative to Tpt (Ac_3) the maximum solubility of niobium in the α_2 phase increases and reaches 8-11% at 800°C [4-7]. A further decrease in temperature is accompanied by decreasing maximum solubility of niobium because of the O phase formation. An increased niobium content in the α_2 phase causes its transformation to the orthorhombic O phase (Figs. 1d).

On the basis of the foregoing, we may represent the evolution of the phase transformations in the alloy with increasing quenching temperature as follows. The initial O phase with a medium niobium content partially decomposes at 800-900°C with the formation of the β (B2) phase. As a result, the niobium content in the O phase decreases, and this phase partially transforms to the α_2 phase, which, upon subsequent quenching, undergoes reverse transformation because it is supersaturated with niobium (Figs. 1e).

Consider the further transformation of the initial O phase during its dissolution. Niobium partially passes into the β phase, and the α_2 phase forms in the regions most depleted of niobium. This is clearly confirmed by the micrograph of a plate (Fig. 1f), whose central region is occupied by the α_2 phase. The α_2

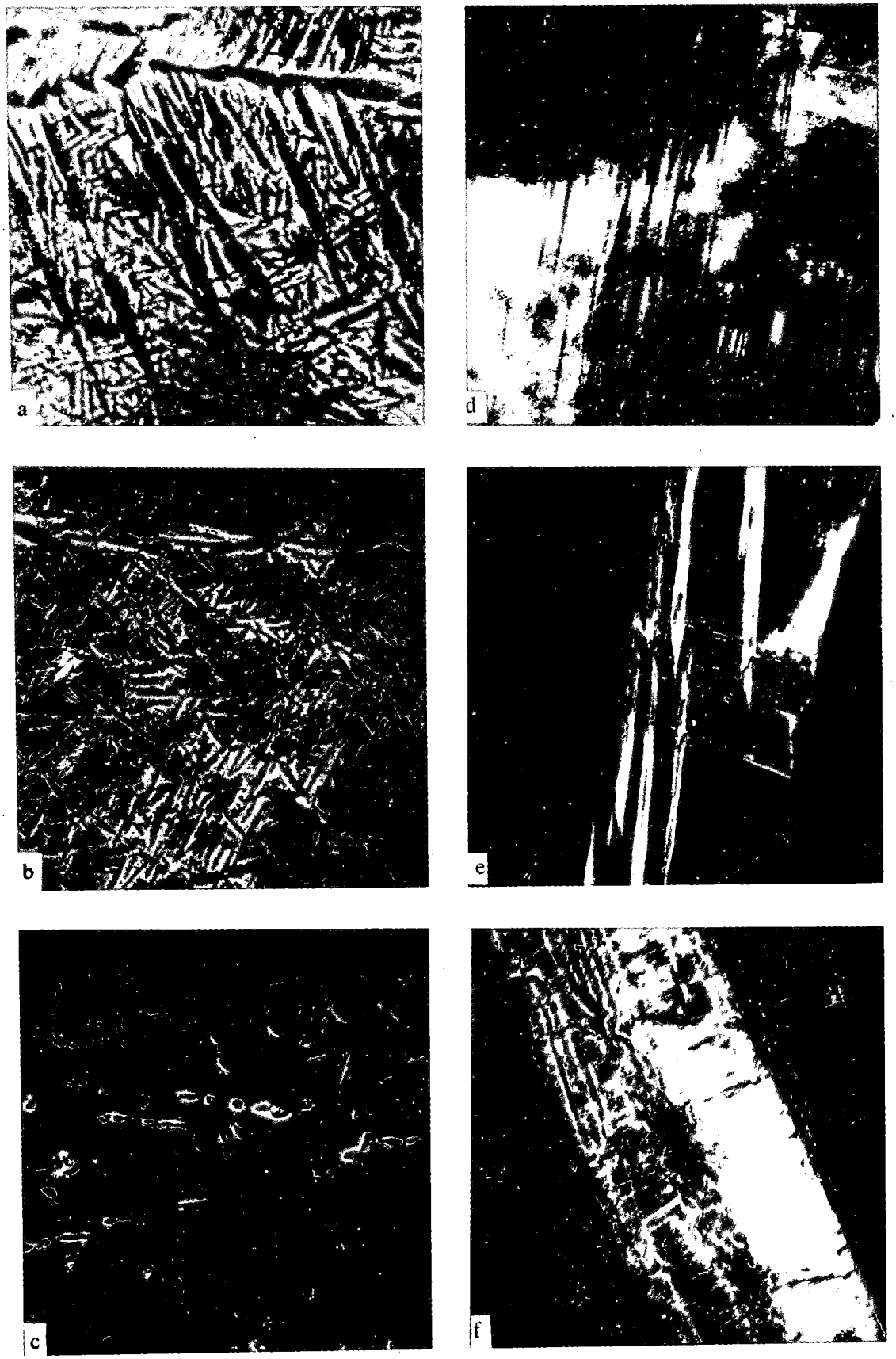

Fig.1. Microstructure of the alloy in the initial and as-quenched states:
a- initial state, SEM,x6000; b- quenching from 1000°C, SEM,5min, x6000; c- quenching from 1100°C SEM,5min, x6000; d- quenching from 900°C, TEM, 30min, x72000; e- quenching from 950°C, TEM (dark field), 30min, x72000; f- quenching from 1000°C ,TEM, 30min, x72000;

phase was identified by selected-area electron diffraction. The doubled reflections are the evidence of matching lattices of the O and α_2 phases. The α_2 phase reflections are represented by points, whereas the O-phase reflections are diffuse in the azimuthal and radial directions, indicating that the O phase composition varies within the plate, and, therefore, the lattice parameter gradually changes, depending on the position in the plate. This means that the occurrence of the phase transformation is always accompanied by the development of a gradient of the concentrations of the alloying elements over the cross section of the plates. The O => α_2 + β transformation is accompanied by the migration of the O/α_2 and O/β interfaces into the O phase, which gradually decreases in size up to complete disappearance. This results in the formation of the α_2 + β structural state (950°C, Fig. 2a).

Changes in the niobium content in the phases may be traced in the vertical polythermal sections of the Ti-Al-Nb ternary phase diagram [6].

Upon cooling, the supersaturated α_2 phase partially transforms to the O phase. The extent of the transformation is determined by the quenching temperature and the time of holding at the quenching temperature. At temperatures above 1000°C, the niobium content in the α_2 phase becomes so small that the high-temperature state of the α_2 phase is completely fixed by cooling (Figs. 2a, 2c).

With increasing quenching temperature, the lattice parameters of the O phase in the as-quenched state approach those of the α_2 phase (Figs. 3a, 3b). This is most pronounced for t = 5 min. At long times of holding at the quenching temperature, the lattice parameters change only insignificantly with the quenching temperature, and the changes in the O phase lattice parameters are virtually similar after holding for 30 min and 1 h. As the holding time increases, the α_2 phase forms at lower temperatures and in a wider temperature range (Fig. 2). This shows that the processes under consideration are controlled by the niobium diffusion from the O phase plates to the β matrix. Therefore, from the structural point of view, the rate of the high-temperature O => α_2 + β transformation is largely determined by the thickness of the initial O phase plates.

An increase in the volume fraction of the β phase with increasing quenching temperature is accompanied by decreasing its lattice parameter (Fig. 3c). The possibility of fixing the metastable β phase by quenching allows us to trace the effect of aluminum on the bee lattice parameter when the aluminum content is sufficiently high. The lattice parameter of the alloy quenched as to retain the β phase was experimentally found to be 0.324 nm. Calculations by Vegard's law predict it to be about 0.327 nm. According to [8], the bcc lattice parameter in the binary Ti-Nb alloys obeys Vegard's law, whereas the Al-Nb and Al-Ti atom pairs exhibit substantial negative deviations from this law (to smaller lattice-parameter values). The calculated data were brought into agreement with the experimental data by using corrections to Vegard's law. The correction for the Al-Ti pair was taken from the data for the hexagonal lattice [8]. The coincidence of the calculated and experimental data confirms the applicability of the correction for both hexagonal and cubic lattices. Thus, the β phase lattice parameter is mainly determined by the aluminum content (the atomic sizes of titanium and niobium are virtually the same). Correspondingly, the aluminum content in the β phase increases and its lattice parameter decreases with increasing quenching temperature (Fig. 3c).

4. CONCLUSIONS

(1) The effects of quenching temperature and the time at quenching temperature on the phase compositions of the α_2 titanium superalloy in the high-temperature and as-quenched states have been determined.

(2) It was found that the O => α_2 + β transformation is controlled by the redistribution of niobium between the phases present in the alloy and, therefore, the transformation rate is determined by the thickness of the initial O phase plates.

(3) The α_2 phase that forms at temperatures below 1000°C completely or partially transforms into the O phase by a displacive mechanism upon subsequent quenching.

(4) With increasing quenching temperature, the niobium content in the O phase decreases, and its lattice parameters gradually approach those of the α_2 phase.

(5) The deviations from Vegard's law for the Ti-Al pair in the hexagonal lattice are also valid for the cubic lattice.

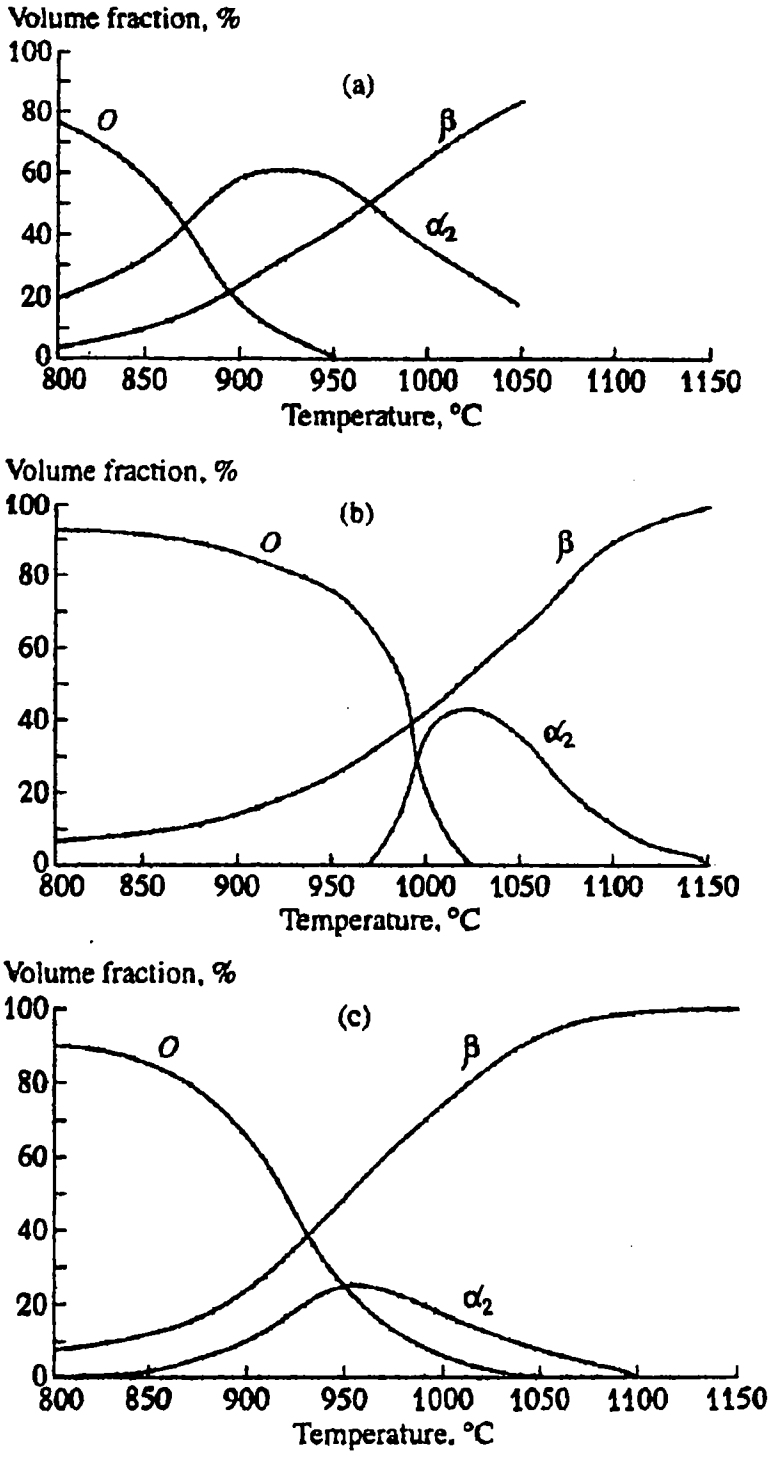

Fig. 2. Phase composition of the alloy as a function of thequenching temperature and time at quenching temperature: a- high-temperature state, holding for 30 min; b- as-quenched state, holding for 5 min; c- as-quenchedstate, holding for 30 min.

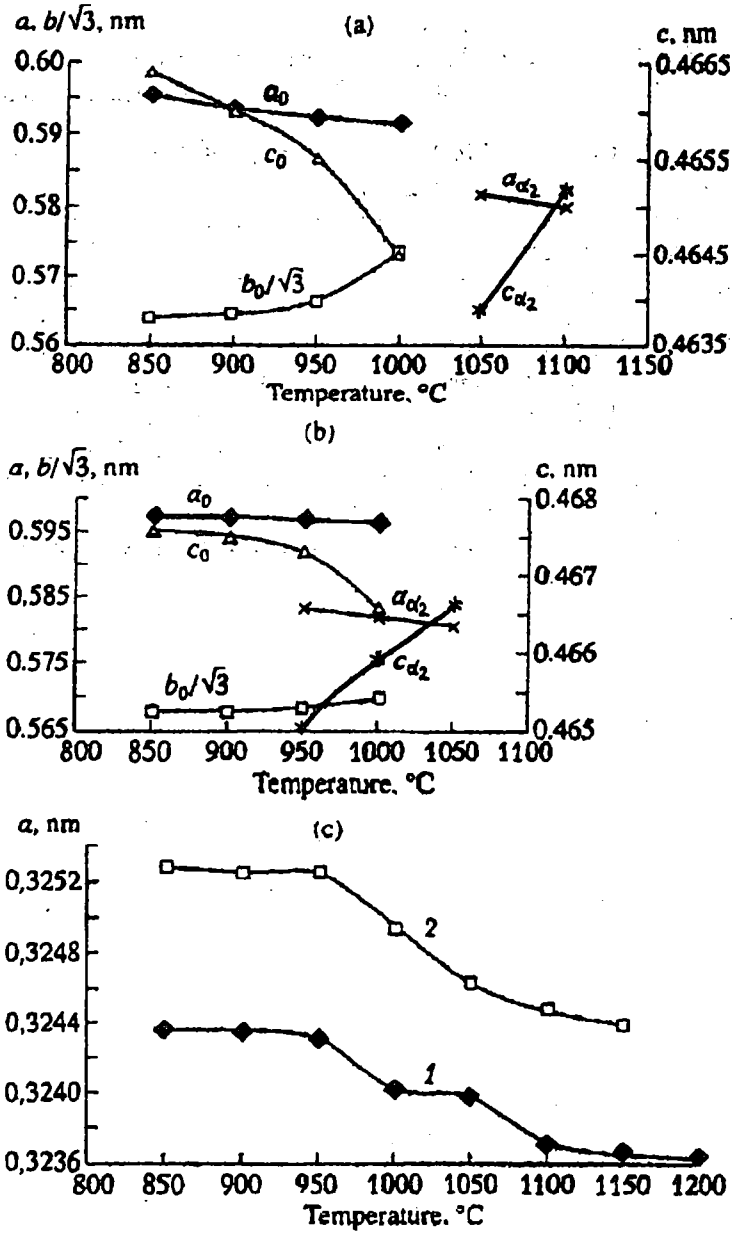

Fig. 3. Lattice parameters of the phases as a function of the quenching temperature: (b) holding for 5 min: (b) holding for 30 min: and (c) p phase, holding for (1) 5 and (2) 30 min.

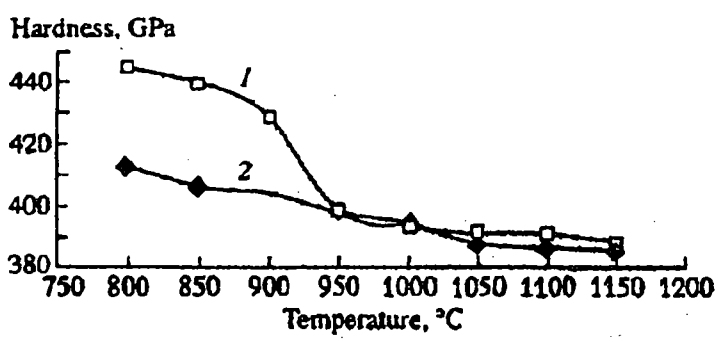

Fig. 4. Hardness of the alloy as a function of the quenching temperature and the holding time: (1) 5 and (2) 30 min.

REFERENCES

1. SUN, L., ZHOU, G., ZHANG, Q., and TOIL, X., The Relationship between Phase and Fracture of Ti_3Al Base Alloys. *Titanium 95: Science and Technology, Proc. 8th WorldConf.*, Birmingham, 1995, pp. 310-315.

2. WARD, C.H., Microstructure Evolution and Its Effect on Tensile and Fracture Behaviour of Ti-Al-Nb α_2 Intermetallics, *Int. Mater. Rev.*, 1993, vol. 38, no. 2, pp. 79-101.

3. HON, W.P., WU, S.K., and KOO, C.H., The Tensile Properties of a Textured $Ti_{65}Al_{25}Nb_{10}$ Alloy, *Mater. Sci. Eng.*, A., 1991, vol. 131, pp. 85-91.

4. MURALEEDHARAN, K., GOGIA, A.K., NANDY, T.K., et al. Transformations in a Ti-24Al-15Nb Alloy. *Metall. Trans.* A, 1992, vol. 23, pp. 401-431.

5. STRYCHOR R., WILLIAMS J.C., and SOFFA W.A., Phase Transformations and Modulated Microstructures in Ti-Al-Nb Alloys, *Metall. Trans.* A, 1988. vol. 19, pp. 225-234.

6. SAGAR, P.K., BANERJEE, D., MURALEEDHARAN, K.. and PRASAD, Y., High-Temperature Deformation Processing of Ti-24Al-20Nb, *Metall. Mater. Trans.* A, 1996, vol. 27, pp. 2593-2604.

7. MURALEEDHARAN K., BANERJEE, D. Alloy Partitioning in Ti-24Al-11Nb by Analytical Electron Microscopy, *MetalL Trans.* A, 1989, vol. 20, pp. 1139-1142.

8. PEARSON, W., The Crystal Chemistry and Physics of Metals and Alloys, New York: Wiley, 1972.